

Accelerating matchmaking of novel dysmorphology syndromes through clinical and genomic characterization of a large cohort

Ranad Shaheen, PhD¹, Nisha Patel, PhD¹, Hanan Shamseldin, MSc¹, Fatema Alzahrani, BSc¹, Ruah Al-Yamany, MD¹, Agaadir ALMoisheer, MSc¹, Nour Ewida, BSc¹, Shamsa Anazi, MSc¹, Maha Alnemer, MD², Mohamed Elsheikh, MD³, Khaled Alfaleh, MD^{3,4}, Muneera Alshammari, MD⁴, Amal Alhashem, MD⁵, Abdullah A. Alangari, MD⁴, Mustafa A. Salih, MD⁴, Martin Kircher, MD⁶, Riza M. Daza, PhD⁶, Niema Ibrahim, BSc¹, Salma M. Wakil, PhD¹, Ahmed Alaqeel, MD⁷, Ikhlas Altowajri, MD⁷, Jay Shendure, MD, PhD⁶, Amro Al-Habib, MD⁷, Eissa Faqieh, MD⁸ and Fowzan S. Alkuraya, MD^{1,9}

Purpose: Dysmorphology syndromes are among the most common referrals to clinical genetics specialists. Inability to match the dysmorphology pattern to a known syndrome can pose a major diagnostic challenge. With an aim to accelerate the establishment of new syndromes and their genetic etiology, we describe our experience with multiplex consanguineous families that appeared to represent novel autosomal recessive dysmorphology syndromes at the time of evaluation.

Methods: Combined autozygome/exome analysis of multiplex consanguineous families with apparently novel dysmorphology syndromes.

Results: Consistent with the apparent novelty of the phenotypes, our analysis revealed a strong candidate variant in genes that were novel at the time of the analysis in the majority of cases, and 10 of these genes are published here for the first time as novel candidates (*CDK9*, *NEK9*, *ZNF668*, *TTC28*, *MBL2*, *CADPS*, *CACNA1H*, *HYAL2*, *CTU2*,

and *C3ORF17*). A significant minority of the phenotypes (6/31, 19%), however, were caused by genes known to cause Mendelian phenotypes, thus expanding the phenotypic spectrum of the diseases linked to these genes. The conspicuous inheritance pattern and the highly specific phenotypes appear to have contributed to the high yield (90%) of plausible molecular diagnoses in our study cohort.

Conclusion: Reporting detailed clinical and genomic analysis of a large series of apparently novel dysmorphology syndromes will likely lead to a trend to accelerate the establishment of novel syndromes and their underlying genes through open exchange of data for the benefit of patients, their families, health-care providers, and the research community.

Genet Med advance online publication 3 December 2015

Key Words: ambiguous genitalia; CHARGE; hypoglycemia; microcephaly; skeletal dysplasia

INTRODUCTION

Although the scope of contemporary clinical genetics has greatly expanded beyond diagnosing rare dysmorphology syndromes, it remains an integral part of a typical clinical genetics practice. These syndromes often represent the pleiotropic effect of single gene mutations, and much has been learned about the function of human genes through the study of these syndromes despite their individual rarity. Pattern recognition is a key skill in the practice of clinical genetics because, although individual dysmorphic features can be part of the normal interindividual variation, it is their combined presence in an individual that prompts the diagnosis of a syndrome.¹ Failure to find a match for the dysmorphology pattern in the published literature may not necessarily indicate the novelty of the syndrome because

the matching process remains a largely subjective approach that is error-prone despite recent efforts toward standardization.² In forums examining such cases (e.g., dysmorphology conferences and small meetings, databases, published literature), researchers often seek to establish that a particular syndrome is truly novel. Unfortunately, this process lacks throughput, and for many patients it is not unusual for many years to pass before they are designated as having a novel recognizable syndrome. Such designation is important, however, because it can be the basis for establishing the molecular pathogenesis and natural history of the disease through the identification of similarly affected patients.

Genotyping first is a recent trend made possible by the advent of genomic tools, initially in the form of genome-wide

N.P., H.S., F.A., and R.A.-Y. contributed equally to this work.

¹Department of Genetics, King Faisal Specialist Hospital and Research Center, Riyadh, Saudi Arabia; ²Department of Obstetrics and Gynecology, King Faisal Specialist Hospital and Research Center, Riyadh, Saudi Arabia; ³Department of Obstetrics and Gynecology, Suliman AlHabib Hospital, Riyadh, Saudi Arabia; ⁴Department of Pediatrics, College of Medicine, King Saud University, Riyadh, Saudi Arabia; ⁵Department of Pediatrics, Prince Sultan Military Medical City, Riyadh, Saudi Arabia; ⁶Department of Genome Sciences, University of Washington, Seattle, Washington, USA; ⁷Department of Surgery, College of Medicine, King Saud University, Riyadh, Saudi Arabia; ⁸Department of Pediatrics, King Fahad Medical City, Riyadh, Saudi Arabia; ⁹Department of Anatomy and Cell Biology, College of Medicine, Alfaisal University, Riyadh, Saudi Arabia. Correspondence: Fowzan S. Alkuraya (falkuraya@Kfshrc.edu.sa)

Submitted 26 May 2015; accepted 3 September 2015; advance online publication 3 December 2015. doi:10.1038/gim.2015.147

copy-number analysis and, more recently, sequencing tools that have the power to identify the likely causal mutation (genotype) regardless of knowledge of the disease (phenotype).^{3,4} Much has been published about the rapidly changing practice of clinical genetics as a consequence of next-generation sequencing technology, and about how the bottleneck has now shifted to identifying phenotypic matches for syndromes in which a novel candidate gene is identified based on a single family. This, in turn, will establish these as recognizable syndromes and facilitate reporting their candidate causal variants in the literature for the benefit of other patients, their caregivers, and the research community at large.^{5,6}

Efforts have been made to accelerate the establishment of novel candidate genes in the literature. For example, we have published the identification of several novel candidate genes in the setting of retinal dystrophy and primordial dwarfism, and some of these genes have since been independently verified by others.⁷⁻⁹ Recently, we published the identification of 33 novel candidate genes for various neurocognitive phenotypes, and at least 6 of these were independently found to be mutated by other investigators in the few months since the article appeared online (unpublished data).¹⁰ However, we are not aware of any similar effort to accelerate the discovery of novel candidate genes specifically in the setting of dysmorphology syndromes. In this article, we describe our experience with members of 31 multiplex consanguineous families who appeared to have novel dysmorphology syndromes at the time of their initial evaluation; 15 of them are reported here for the first time. Genomic analysis of this cohort revealed novel disease candidates, and their reporting should facilitate “match-making” among the wider clinical genetics community.

MATERIALS AND METHODS

Human subjects

Patients were evaluated as part of a standard clinical genetics evaluation by board-certified clinical geneticists. Eligible patients were those with an apparently novel phenotype involving, but not limited to, facial dysmorphism or skeletal dysplasia, positive family history consistent with autosomal recessive inheritance, and consanguineous parents. Two families (families 14 and 15) did not meet these criteria but were included because they have a clinical phenotype similar to that of family 13 (see below). Informed consent was obtained from all subjects prior to enrollment under an institutional review board–approved research protocol (KFSHRC RAC#2080006). Venous blood was collected in ethylenediaminetetraacetic acid for DNA extraction, and clinical photographs were taken after obtaining a separate photo consent form.

Autozygome analysis

Determination of the entire set of autozygous intervals per genome (autozygome) was as previously described.¹¹ Briefly, we genotyped DNA samples using Axiom SNP Chip according to the manufacturer’s instructions (Affymetrix), followed by a

genome-wide search for autozygous intervals using regions of homozygosity of >1 Mb as surrogates on AutoSNPa.¹² When multiple affected members were available, their shared autozygome was determined.¹³

Whole-exome and whole-genome sequencing

Exome capture was performed using a TruSeq Exome Enrichment kit (Illumina, San Diego, CA) following the manufacturer’s protocol. Samples were prepared as an Illumina sequencing library; in the second step, the sequencing libraries were enriched for the desired target using the Illumina Exome Enrichment protocol. The captured libraries were sequenced using Illumina HiSeq 2000 Sequencer. The reads are mapped against UCSC hg19 (<http://genome.ucsc.edu/>) by Burrows-Wheeler Aligner (BWA) (<http://bio-bwa.sourceforge.net/>). The SNPs and Indels were detected by SAMTOOLS (<http://samtools.sourceforge.net/>). For whole-genome sequencing, amplification-free Illumina TrueSeq libraries were prepared, pooled, and then sequenced on six different Illumina HiSeq runs. Full-length paired-end reads were aligned using Burrows-Wheeler Aligner (BWA) MEM to Homo sapiens GRCh37 reference sequence (1000 Genomes Project phase 2: <http://www.1000genomes.org/>) with default parameters. BWA output was directly BAM-converted and genomic coordinate-sorted, and then subjected to a GATK insertion/deletion realignment process. We obtained average genome coverage of $13.11\times$ ($5\times$: 0.9590, $10\times$: 0.7338, $15\times$: 0.3022). Variants were called using both GATK’s UnifiedGenotyper 3.2-2 and HaplotypeCaller 3.2-2. Both sets were filtered to remove variants that were present in more than 50% of individuals, those with less than three reads coverage, and those with more than 2.5% minor allele frequency in 1000 Genomes phase 3 release or the Exome Variant Server (<http://evs.gs.washington.edu/EVS/>). For both whole-exome and whole-genome sequencing, the candidacy of the resulting variants was based on their physical location within the autozygome of the affected individual, their population frequency, and the predicted effect on the protein as described previously.^{10,14}

RESULTS

Clinical characterization of apparently novel dysmorphology syndromes

Each of the 31 study families had a unique set of dysmorphic features and other systemic manifestations that did not appear to fit a previously recognized syndrome at the time of the analysis (Table 1 and Figure 1; Supplementary Table S1 online). Family pedigrees for the 15 families reported here for the first time are shown in Figure 2. In some families—e.g., 11DG0424, 14DG1221, and 11DG0268—there was a sufficient number of affected and unaffected members to map the phenotype to a single novel locus each, thus confirming the novelty of the phenotype even before exome sequencing. In most families, however, novelty of the phenotype could be verified only after exome sequencing.

Table 1 Summary of the study cohort

Family ID	Lab ID	Total size of ROH (Mb)	Size range of ROH (Mb)	Size of ROH spanning the candidate gene (Mb)	Clinical descriptions	Reference
Family 1	11DG0424, 11DG1630	20	—	20	Microcephaly, coloboma, cataract, renal anomalies, abnormal genitalia, congenital heart disease, club foot, global developmental delay, and dysmorphism (CHARGE-like)	This study
Family 2	13DG0784	277	2–67	67	Severe failure to thrive, coloboma, brain atrophy, osteopenia, congenital heart disease, global developmental delay, polysplenia, and marked facial dysmorphism	This study
Family 3	10DG1767, 10DG1768, 10DG1769	13	1–8	8	Retinal dystrophy, myopia, short stature, skeletal dysplasia, and congenital heart disease (later found to represent a mild form of Jeune asphyxiating thoracic dystrophy)	This study
Family 4	08DG00382, 08DG00384	199	1–66	7	Mild developmental delay, marked joint laxity with recurrent fractures and subluxation, and mild facial dysmorphism	This study
Family 5	10DG0648, 10DG1459, 10DG1460	52	1–23	4	Progressive ataxia, developmental delay, and facial dysmorphism	This study
Family 6	12DG1638, 12DG2364, 12DG2365	27	10–17	17	Severe syndactyly, variable pterygium formation, anal stenosis and mild facial dysmorphism	This study
Family 7	14DG1447, 14DG1448	25	4–7	4	Craniosynostosis, developmental delay, and mild hepatomegaly	This study
Family 8	13DG0792, 13DG0793	96	1–12	11	Hepatic cysts with ductal malformation, bilateral polycystic kidney with renal failure, mild skeletal dysplasia, and cerebellar hypoplasia	This study
Family 9	13DG0916, 15DG0234	98	1–20	14	Global developmental delay, epilepsy, recurrent nonketotic hypoglycemia (in two of three siblings), and facial dysmorphism (including cleft palate in two of three siblings)	This study
Family 10	12DG1565, 12DG1566	146	3–55	10	Ptosis and facial dysmorphism	This study
Family 11	14DG1221, 15DG1187	21	—	21	High myopia, short stature, and facial dysmorphism (hypertelorism in both and cleft lip and palate in one)	This study
Family 12	13DG1395	154	1–22	—	Perinatal lethality, microcephaly, radial ray deficiency, and other skeletal abnormalities, severe facial dysmorphism (including cleft in one of the two siblings)	This study
Family 13	14DG0993, 15DG0395	75	3–8	8	Microcephaly, unilateral renal agenesis, congenital heart disease, agenesis of corpus callosum, and facial dysmorphism	This study
Family 14	14DG1883	76	1–18	2	Microcephaly, brachycephaly, facial dysmorphism, congenital heart diseases, and ambiguous genitalia	This study
Family 15	12DG0529	52	1–8	4	Microcephaly, facial dysmorphism, lissencephaly, congenital skeletal abnormalities, unilateral renal agenesis, ambiguous genitalia, and micropenis	This study
Family 16	15DG0764, 15DG0765	42	2–20	20	Macrocephaly, facial dysmorphism, cerebral calcifications, hypotonia, skeletal dysplasia, generalized skin, and joint laxity and hernia	This study
Family 17	14DG0805	213	2–34	13	Facial dysmorphism, holoprosencephaly, unilateral absent radius, and pulmonary atresia	This study
Family 18	10DG0300, 10DG0301, 10DG0538	45	17–29	29	Arthrogryposis, upward gaze palsy, Perthes disease, uncontrolled bronchial asthma, subtle facial dysmorphism, and pyloric stenosis (in two out of the three family members)	This study/ PMID: 21271645
Family 19	10DG1175	24	1–17	17	Global developmental delay, microcephaly, truncal obesity, and dysmorphic facies	PMID: 25558065
Family 20	08DG00469	12	—	12	Severe intellectual disability, hirsutism, dysmorphic facies, and skeletal abnormalities	PMID: 20950399
Family 21	12DG0685	358	1–46	46	Intellectual disability, dysmorphic facies, and pulmonary stenosis (Noonan-like)	PMID: 25558065
Family 22	11DG0502 & 13DG0056	61	1–13	8	Global developmental delay, dysmorphic facies, and brain atrophy	PMID: 25558065

ROH, region of homozygosity.

Table 1 Continued on next page

Table 1 Continued

Family ID	Lab ID	Total size of ROH (Mb)	Size range of ROH (Mb)	Size of ROH spanning the candidate gene (Mb)	Clinical descriptions	Reference
Family 23	12DG1149	180	2–36	—	Intellectual disability, dysmorphic facies (Robinow-like), bifid scrotum, and undescended testes	PMID: 25558065
Family 24	08DG00198	10	—	10	Global developmental delay, dysmorphic facies, and abnormal glycosylation (CDG IIa)	PMID: 20684000
Family 25	11DG0932, 11DG0933, 11DG0936	153	1–26	26	Global developmental delay and dysmorphic facies	PMID: 25558065
Family 26	12DG1306	256	1–101	101	Proptosis, dysmorphic facies and dwarfism	PMID: 24389050
Family 27	11DG0268	2	—	2	Intellectual disability and hypohidrosis	PMID: 23606727
Family 28	09DG0658	23	—	23	Dysmorphic facies and dwarfism	PMID: 22840364
Family 29	10DG1670	42	1–33	33	Global developmental delay, epilepsy, and facial dysmorphism	PMID: 25558065
Family 30	12DG2241, 13DG2294	120	1–32	3	Global developmental delay (with severe intellectual disability), dysmorphic features, hyperactivity with autistic behavior, and agenesis of corpus callosum	PMID: 23620220
Family 31	10DG0934	18	1–5	2	Dysmorphic facies, cerebellar vermis hypoplasia, Dandy-Walker malformation, hydrocephalus, congenital heart disease, and developmental delay	PMID: 21567916/ PMID: 25558065
Family 32	13DG0538	328	1–51	44	Facial dysmorphism, lens dislocation, anterior-segment abnormalities, and spontaneous filtering blebs	PMID: 24768550
Family 33	08DG00246	3	—	3	Facial dysmorphism, Klippel-Feil anomaly, and myopathy	PMID: 25748484

ROH, region of homozygosity.

High yield of autozygome/exome analysis for dysmorphology syndromes in multiplex consanguineous families

A strong candidate variant was identified in 90% (28/31) of the study cohort (Tables 2 and 3). At a minimum, the causal variant must have been the only novel homozygous coding/splicing variant predicted to be pathogenic within the shared autozygome of the affected members of the respective family. In the remaining three families more than one variant remained, so we classified them as “unsolved.” Segregation of the variants was confirmed by Sanger sequencing among all available family members.

Consistent with the clinical impression that the phenotypes in this cohort are novel, only 19% (6/31) were found to have the strong candidate mutation in a known disease gene (Table 3). In some families, this is because the previously published gene had an extremely limited phenotypic description. For example, family 21 (12DG0685) had a distinct constellation of features but their underlying disease gene *ZNF526* was described only in the context of intellectual disability, with very few clinical details.¹⁵ In another family—family 24 (08DG00198)—the dysmorphology profile fit a recognizable but very rarely described syndrome, CDGIIa. Similarly, family 7 (14DG1447), which had a homozygous truncating mutation in *MAN2B1*, presented with nonspecific developmental delay and severe craniosynostosis. Craniosynostosis has very rarely been described in

mannosidosis, so this diagnosis was not considered initially (Supplementary Figure S4 online). Finally, the phenotype for some genes was sufficiently different from what has been described in the literature that it was not possible to recognize them clinically. This includes family 3 (10DG1767), with members who presented with narrow chest and myopia and were later found to have cone-rod dysfunction. These members mapped to two autozygous intervals, neither of which appeared to contain a good candidate. Exome sequencing did not reveal any candidate coding/splicing variant. Close examination of the known disease genes within the two critical intervals highlighted *C21orf2*, an established disease gene for cone-rod dystrophy.⁷ Interestingly, one of the two *C21orf2*-linked cone-rod dystrophy families that we had originally described⁷ was found on careful examination to display short stature and narrow chest whereas the other was completely nonsyndromic. Thus, *C21orf2* appears to cause both syndromic and nonsyndromic cone-rod dysfunction. We therefore carefully considered all novel homozygous variants in *C21orf2* and identified a deep intronic mutation, which we confirmed as impairing normal splicing (Supplementary Figure S2 online). Similarly, family 27 (11DG0268) mapped to a single locus containing the known disease gene *COG6*, but the phenotype (intellectual disability and anhidrosis) was very different from the published *COG6*-related CDG phenotype, as we described in detail elsewhere.^{16,17}



Figure 1 Representative clinical images of the study subjects. (a) Clinical photograph for case 11DG0424 (family 1) showing microcephaly, coloboma, and prominent nasal bridge. (b) Clinical photograph for case 13DG0784 (family 2) showing very large ears, large nose, and deep-set eyes. (c) Clinical photograph for case 10DG1767 (family 3) showing a narrow chest with pectus carinatum. (d) Clinical photograph for case 10DG0648 (family 5) showing the deviated nasal septum and strabismus. (e) Clinical photograph for case 14DG1447 (family 7) showing retracted upper face, down-slanting palpebral fissures, and small nose. (f) Clinical photograph for case 13DG0916 (family 9) showing upturned nose and tented upper lip. (g) Clinical photograph for case 12DG1565 (family 10) showing unilateral left ptosis, hypoplastic maxilla, short upturned nose, and tented upper lip. (h) Clinical photograph for case 14DG1221 (family 11) showing hypertelorism, strabismus, hypoplastic maxilla, micrognathia, low-set ears, and broad nose. (i) Clinical photograph for case 13DG1395 (family 12) showing severe microcephaly, hypertelorism, malar hypoplasia, low-set ears, wide nasal bridge, and bilateral cleft lip and palate. (j) Clinical photograph for case 14DG0993 (family 13) showing a stillborn boy with severely hypoplastic nose and abnormal genitalia. (k) Clinical photograph for case 15DG0764 (family 16) showing macrocephaly and bulbous nose. (l) Clinical photograph for case 10DG1175 (family 19) showing synophrys, deep-set eyes, bulbous nose, and prominent cheeks. (m) Clinical photograph for case 12DG0685 (family 21) showing hypoplastic maxilla and macrostomia with full lips. (n) Clinical photograph for case 11DG0502 (family 22) showing bilateral exophthalmos, strabismus, upturned nares, and long philtrum. (o) Clinical photograph for case 12DG1149 (family 23) showing severe ocular hypertelorism with mild synophrys and arched bushy eyebrows, infra-orbital creases, and depressed nasal bridge. (p) Clinical photograph for case 10DG1670 (family 29) showing full lips and prominent philtrum. (q) Clinical photograph for case 14DG0805 (family 17) showing severe microtia (upper limb deformity caused by absent radius is not visible). (r) Radiological image for case 08DG00384 (family 4) showing bilateral knee dislocation. (s) Radiological image of 13DG0792 (family 8) showing acromelia and metaphyseal and distal digital changes. (t) Clinical photograph of case 12DG1638 (family 6) showing severe syndactyly of the fingers.

In 67% (21/31) of families, the strong candidate variant was identified in a gene that was novel at the time of analysis. These include 11 genes that we published previously¹⁰ and 10 that we describe for the first time here (Table 2).

Family 1 (11DG0424 and 13DG2294) consists of two cousins with a strikingly similar phenotype that is best described as CHARGE-like. They both had coloboma, renal malformation,

restricted growth, and limb anomalies (Figures 1 and 2; Supplementary Table S1 online). A single autozygous interval was exclusively shared by the two affected corresponding to chr9:111,576,346-132,018,909, and therein the only novel candidate variant was a missense variant in *CDK9* (NM_001261.3: c.673C>T; p.Arg225Cys, PolyPhen=probably damaging (0.913), Sorting Intolerant From Tolerant

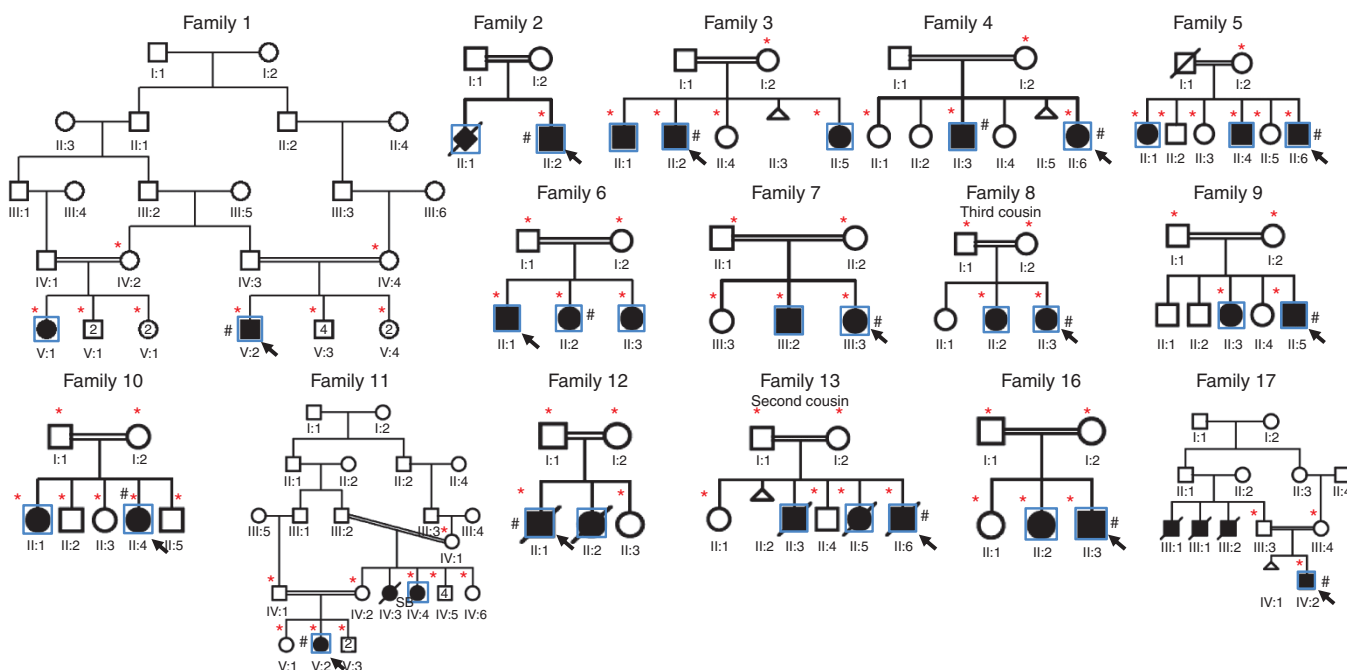


Figure 2 Pedigrees for the 15 families described for the first time in this article. The index is indicated in each pedigree by a black arrow. Asterisks denote individuals whose DNA was available for analysis and segregation. Blue boxes indicate the cases that were clinically evaluated. The hash tag (#) denotes individuals whose DNA was exome-sequenced.

(SIFT)=deleterious (0.05)) (Supplementary Figure S1 online; Tables 1 and 2).

Family 2 (13DG0784) has a highly unusual dysmorphic syndrome characterized by very large ears, deep-set eyes, and severe developmental delay and growth deficiency (Figure 1; Supplementary Figure S2 online). The homozygous truncating variant in *ZNF668* (NM_001172668.1:c.955C>T; p.Gln319*) was the only novel candidate within the autozygome of the index (Table 2).

Family 4 (08DG00382 and 08DG00384) consists of two siblings with an apparently unique form of skeletal dysplasia with multiple joint dislocation (Figure 1; Supplementary Figure S2 online). Exome sequencing in both siblings failed to identify a mutation in any of the genes known to cause skeletal dysplasia but revealed a novel missense variant in *TTC28* (NM_001145418.1:c.1462G>A; p.Gly488Ser; PolyPhen=probably damaging (0.973); SIFT=deleterious (0)) as the only novel coding/splicing variant within the shared autozygome (Table 2).

Family 5 (10DG0648, 10DG1459, and 10DG1460) consists of four affected siblings with progressive ataxia, developmental delay, and facial dysmorphism (Figures 1 and 2; Supplementary Figure S3 and Table S1 online). Exome sequencing of one sibling did not reveal any novel variant within the shared autozygome between the three living affected siblings. Therefore, we proceeded with WGS, which revealed a homozygous microdeletion of 15,500 bp (hg19, chr13:96,442,001-96,457,500) that includes part of intron 11, exon 12, and the 3-untranslated region of *DNAJC3* and part of the 3-untranslated region of *UGTT2* (Supplementary Figure S3 online; Table 2). Synofzik *et al.*¹⁸ recently reported that *DNAJC3* mutations cause

progressive ataxia and neurodegeneration; therefore, this gene is not included among the 10 novel genes in this study.

Family 6 (12DG1638, 12DG2364, and 12DG2365) consists of a boy and his two sisters with severe syndactyly and variable penetrance of multiple pterygium (Figures 1 and 2; Supplementary Figure S4 and Table S1 online). Three autozygous intervals (chr10:49,083,380-64,516,338, chr3:116,530,905-133,802,238 and chr11:95,069,943-105,483,626) were exclusively shared by the affected siblings. Exome sequencing revealed a large genomic deletion within the first locus that completely removes *MBL2*, which was further confirmed by high-resolution molecular karyotyping (Supplementary Figure S4 online). No other novel variants were identified by exome in either of the two remaining autozygous intervals.

Family 9 (13DG0916 and 15DG0234) consists of three siblings who presented with global developmental delay and variable penetrance of cleft palate and hypoglycemia (Figure 1; Supplementary Figure S5 and Table S1 online). The splicing variant identified by exome sequencing in *CADPS* (NM_003716.3:c.442-1G>C) was the only novel coding/splicing variant within the shared autozygome of the two siblings who were alive. Reverse-transcription polymerase chain reaction (RT-PCR) using a patient-derived lymphoblastoid cell line confirmed that this homozygous mutation was truncating (p.Ile148Glnfs*24) (Supplementary Figure S5).

Family 10 (12DG1565 and 12DG1566) consists of two sisters with ptosis and facial dysmorphism (Figure 1; Supplementary Figure S6 online). Exome sequencing revealed a homozygous truncating mutation in *CACNA1H* as the only novel coding/splicing variant within the shared autozygome (Table 2).

Table 2 Variants identified in novel genes at the time of analysis

Candidate gene	Family ID	Lab ID	Candidate variant	Variant type/bioinformatics prediction/pathogenesis evidence	Categorization	Reference
<i>ADAT3</i>	Family 30	12DG2241, 13DG2294	NM_138422.2:c.430G>A; p.Val144Met	Missense: PolyPhen: probably damaging (0.998). SIFT: deleterious (0.01). PHRED: 24.4	Novel gene at the time of WES	PMID: 23620220
<i>ASPH</i>	Family 32	13DG0538	NM_004318.3:c.1852_1856delinsGGG; p.Asn618Glyfs*20	Deletion	Novel gene at the time of WES	PMID: 24768550
<i>C11ORF46</i>	Family 19	10DG1175	NM_152316.2:c.653G>A; p.Gly218Glu	Missense: PolyPhen: probably damaging (1). SIFT: deleterious (0). PHRED: 33	Novel gene at the time of WES	PMID: 25558065
<i>C3ORF17</i>	Family 16	15DG0764, 15DG0765	NM_015412.3:c.280C>T; p.Arg94Cys	Missense: PolyPhen: probably damaging (1). SIFT: deleterious (0). PHRED: 35	Novel gene	This study
<i>CACNA1G</i>	Family 20	08DG00469	NM_198382.2:c.667_669del; p.Phe223del	Deletion	Novel gene at the time of WES	PMID: 20950399
<i>CACNA1H</i>	Family 10	12DG1565, 12DG1566	NM_021098.2:c.1654C>T; p.Arg552*	Nonsense	Novel gene	This study
<i>CADPS</i>	Family 9	13DG0916 and 15DG0234	NM_003716.3:c.442-1G>C; p.Ile148Glnfs*24	Splice site/RT-PCR	Novel gene	This study
<i>CDK9</i>	Family 1	11DG0424, 11DG1630	NM_001261.3:c.673C>T; p.Arg225Cys	Missense: PolyPhen: probably damaging (0.913). SIFT: deleterious (0.05). PHRED: 33	Novel gene	This study
<i>CRIP1</i>	Family 26	12DG1306	NM_014171.4:c.133_134insGG; p.A45Gfs*87	Nonsense	Novel gene at the time of WES	PMID: 24389050
<i>CTU2</i>	Family 13	14DG0993, 15DG0395	NM_001012762.1:c.873G>A; p.(=)	Splice site/RT-PCR	Novel gene	This study
<i>CTU2</i>	Family 14	14DG1883	NM_001012762.1:c.873G>A; p.(=)	Splice site/RT-PCR	Novel gene	This study
<i>CTU2</i>	Family 15	12DG0529	NM_001012762.1:c.873G>A; p.(=)	Splice site/RT-PCR	Novel gene	This study
<i>DNAJC3</i>	Family 5	10DG0648, 10DG1459, 10DG1460	NC_000013.10:g.96442001_96457500del (GRCh37(hg19)); NM_020121.3:c.4529-3434_*12043del, NM_006260.3:c.1358-1126_*14216del	Whole gene deleted	Novel gene at the time of WES	This study
<i>DPH1</i>	Family 31	10DG0934	NM_001383.3:c.701T>C; p.Leu234Pro	Missense: PolyPhen: probably damaging (0.998). SIFT: deleterious (0). PHRED: 27.4	Novel gene at the time of WES	PMID: 21567916/ PMID:25558065
<i>HYAL2</i>	Family 11	14DG1221, 15DG1187	NM_033158.4:c.749C>T; p.Pro250Leu	Missense: PolyPhen: probably damaging (1). SIFT: deleterious (0). PHRED: 26.6	Novel gene	This study
<i>MBL2</i>	Family 6	12DG1638, 12DG2364, 12DG2365	NC_000010.10:g.54337730_54933961del ((GRCh37(hg19)); NM_000242.2:c.-402566_*190167del (complete gene deletion)	Whole gene deleted	Novel gene	This study
<i>MYO18B</i>	Family 33	08DG00246	NM_032608.5:c.6905C>A; p.Ser2302*	Nonsense	Novel gene at the time of WES	PMID: 25748484
<i>NEK9</i>	Family 18	10DG0300, 10DG0301	NM_033116.4:c.2042G>A; p.Arg681His	Missense: PolyPhen: probably damaging (0.999). SIFT: deleterious (0). PHRED: 35	Novel gene	This study/PMID: 21271645
<i>POC1A</i>	Family 28	09DG0658	NM_015426.4:c.241C>T; p.Arg81*	Nonsense	Novel gene at the time of WES	PMID: 22840364
<i>TAF6</i>	Family 25	11DG0932, 11DG0933, 11DG0936	NM_001190415.1:c.323T>C; p.Ile108Thr	Missense: PolyPhen: benign (0.31). SIFT: deleterious (0). PHRED: 23.4	Novel gene at the time of WES	PMID: 25558065

SIFT, Sorting Intolerant From Tolerant; WES, whole-exome sequencing.

Table 2 Continued on next page

Table 2 Continued

Candidate gene	Family ID	Lab ID	Candidate variant	Variant type/bioinformatics prediction/pathogenesis evidence	Categorization	Reference
<i>TBCK</i>	Family 29	10DG1670	NM_033115:c.1708+1G>A	Splice site	Novel gene at the time of WES	PMID: 25558065
<i>TTC28</i>	Family 4	08DG00382 08DG00384	NM_001145418.1:c.1462G>A; p.Gly488Ser	Missense: PolyPhen: probably damaging (0.973). SIFT: deleterious (0.02). PHRED: 27.7	Novel gene	This study
<i>Unsolved (>1 variants)</i>	Family 17	14DG0805	NM_145201.5:c.145C>T: p.Pro49Ser	Missense: PolyPhen: probably damaging (0.999). SIFT: deleterious (0)	<i>Unsolved</i>	This study
<i>NAPRT1</i>			NM_005786.5:c.1279C>T:p.Pro427Ser	Missense: PolyPhen: possibly damaging (0.883). SIFT: tolerated (0.11). PHRED: 23.1		
<i>TSHZ1</i>			NM_002467.4:c.663G>T:p.Lys221Asn	Missense: PolyPhen: probably damaging (0.992); SIFT: tolerated (0.4)		
<i>MYC</i>						
<i>Unsolved (>1 variant)</i>	Family 12	13DG1395	NM_016452:c.1579+2T>G	Splice site	Unsolved	This study
<i>CAPN9</i>			NM_016452:c.1726C>T:p.Arg576Trp	Missense: PolyPhen: benign (0.339). SIFT: deleterious (0). PHRED: 32		
<i>CAPN9</i>			NM_001166105:c.8G>T:p.Arg3Leu	Missense: PolyPhen: benign (0.195). SIFT: deleterious (0). PHRED: 26.4		
<i>TADA2A</i>			NM_020405:c.1223G>A:p.Gly408Asp	Missense/splicing: PolyPhen: benign (0.195). SIFT: tolerated (0.25). PHRED: 22		
<i>PLXDC1</i>						
<i>Unsolved (>1 variants)</i>	Family 23	12DG1149	<i>NDUFC2</i> :NM_001204055.1:c.61C>T; p.Pro21Ser <i>CDH11</i> :NM_001797:c.999+1G>T	Missense: PolyPhen: probably damaging (0.94). SIFT: deleterious (0). PHRED: 29.7	Unsolved	PMID: 25558065
<i>NDUFC2</i>				Splice site		
<i>CDH11</i>						
<i>WWOX</i>	Family 22	11DG0502, 13DG0056	NM_016373.3:c.606-1G>A	Splice site	Novel gene at the time of WES	PMID: 25558065
<i>ZNF668</i>	Family 2	13DG0784	NM_001172668.1:c.955C>T; p.Gln319*	Nonsense	Novel gene	This study

SIFT, Sorting Intolerant From Tolerant; WES, whole-exome sequencing.

Family 11 (14DG1221 and 15DG1187) consists of two affected members who presented with severe hypertelorism, high myopia, and, in one of the two, cleft lip and palate (**Figure 1**; **Supplementary Figure S6** and **Table S1** online). A single autozygous interval (chr3:40899164-54379802) was exclusively shared by the two patients, in whom a missense variant in *HYAL2* was identified (NM_033158.4:c.749C>T; p.Pro250Leu; PolyPhen=probably damaging (1); SIFT=deleterious (0)) (**Supplementary Figure S6** online; **Table 2**).

Family 13 (14DG0993 and 15DG0395) consisted of three affected members with a unique syndrome characterized by facial dysmorphism, severe primary microcephaly with agenesis of corpus callosum, renal agenesis, congenital heart disease, and abnormal genitalia (**Supplementary Figure S7** and **Table S1** online). The index was exome-sequenced, and a homozygous synonymous variant (*CTU2*: NM_001012762.1:c.873G>A)

was the only surviving variant that linked to the shared regions of homozygosity between two of the affected members. Subsequently, two additional families (families 14 and 15) with a nearly identical phenotype were recruited. The index from each of these two families was exome-sequenced and analyzed independently. Exome filtering revealed the same *CTU2* variant as in family 13. Furthermore, the variant was linked to the only autozygous region shared between the affected members in the three families (chr16:88,155,503-89,588,896) with linkage LOD score of 4.5. RT-PCR revealed that the synonymous variant impairs the normal splicing with resulting frameshift and the introduction of a premature stop codon (NM_001012762.1: p.Thr247Alafs*21) (**Supplementary Figure S8** online).

Family 16 (15DG0764 and 15DG0765) consisted of two affected members who presented with

Table 3 Variants identified in known genes

Candidate gene	Family ID	Lab ID	Candidate variant	Bioinformatics prediction	Categorization	Reference
<i>C21ORF2</i>	Family 3	10DG1767, 10DG1768 10DG1769	NM_001271441.1:c.1000-23A>T;	Splice site/RT-PCR	Known disease gene, novel phenotype	This study
<i>COG6</i>	Family 27	11DG0268	NM_020751.2:c.1167-24A>G	Splice site/RT-PCR	Known candidate gene, novel phenotype	PMID: 23606727
<i>MAN2B1</i>	Family 7	14DG1447, 14DG1448	NM_000528.3:c.2402dupG; p.Ser802Glnfs*129	Frameshift	Known disease gene, unrecognized phenotype	This study
<i>MGAT2</i>	Family 24	08DG00198	NM_002408.3:c.711G>C; p.Lys237Asn	Missense: PolyPhen: probably damaging (0.998). SIFT: deleterious (0). PHRED:25.1	Known disease gene, unrecognized phenotype	PMID: 20684000
<i>WDR35</i>	Family 8	13DG0792, 13DG0793	NM_001006657.1:c.206G>A; p.Gly69Asp	Missense: PolyPhen: probably damaging (1). SIFT: deleterious (0). PHRED: 33	Known disease gene, unrecognized phenotype	This study
<i>ZNF526</i>	Family 21	12DG0685	NM_133444.1:c.479A>C; p.Lys160Thr	Missense: PolyPhen: possibly damaging (0.506). SIFT: tolerated (0.06). PHRED: 14.68	Known candidate published, unrecognized phenotype	PMID: 25558065

macrocephaly, hypoplastic maxilla, and skeletal dysplasia (**Figure 1**; **Supplementary Figure S9** online). Exome sequencing revealed a homozygous missense mutation in *C3ORF17* (NM_015412.3:c.280C>T; p.Arg94Cys) as the only novel coding/splicing variant within the shared autozygome.

Family 18 (10DG0300, 10DG0301, and 10DG0538) was previously published based on an apparently novel phenotype consisting of joint contracture, limited upward gaze, and Legg–Calvé–Perthes disease.¹⁹ Exome sequencing revealed a novel missense variant in *NEK9* (NM_033116.4:c.2042G>A; p.Arg681His, PolyPhen=probably damaging (0.999), SIFT=deleterious (0); **Table 2**).

DISCUSSION

We have previously shown that the combined use of autozygome/exome analysis in the setting of multiplex consanguineous families has a diagnostic yield of 75% for neurocognitive phenotypes and 81% for retinal dystrophies.^{7,10} This prompted us to examine the yield of this approach for dysmorphology syndromes in the same setting, i.e., multiplex consanguineous families. Another reason for limiting our study to multiplex families is that the presence of more than one affected individual with the same apparently novel phenotype facilitates the recognition of the core phenotypic features of the syndrome, notwithstanding the known phenomenon of clinical variability. Using this approach, we show that the yield was also high at 91%.

Very recently, Bloss *et al.*²⁰ published their experience with 17 families in which the proband appeared to have novel phenotypes. Subsequent whole-exome sequencing revealed a strong candidate mutation in 60%, including five novel candidate genes and four known disease genes. However, with the exception of one case with suspected Opitz G/BBB, none of the patients reported by Bloss *et al.* had a dysmorphology syndrome. In addition, several of the probands lacked family history, so nongenetic causes (at least in the Mendelian sense) could not be ruled out. Therefore, our study is distinct from the one by Bloss *et al.* in two main aspects. First, a likely mode of inheritance (autosomal recessive)

was present in all of our study families. This may explain, at least in part, the higher yield of our study compared with that by Bloss *et al.* because this has also been shown in a recent review by the Centers of Mendelian Genomics.²¹ However, we note here that we cannot exclude the possibility of dual diagnosis and the presence of more than one underlying causal mutation in consanguineous pedigrees as described recently.²² Second, a distinct dysmorphology profile is present in each of the study families, and this will be much more likely to facilitate “matchmaking” as compared with some of the nonspecific phenotypes reported by Bloss *et al.* (e.g., developmental delay and muscle atrophy).

Despite our best effort to label a dysmorphology phenotype as novel only after an extensive literature search, we note that six study families were found to have mutations in known genes. In the case of *MGAT2*, we have previously shown that this is probably due to the poor documentation of dysmorphology in the metabolic literature.^{13,16,23,24} Similarly, we note that the craniosynostosis we observed in the setting of mild global developmental delay in the two siblings with *MAN2B1* mutation was initially considered a novel phenotype for the same reason. Although craniosynostosis is not listed as a known feature of mannosidosis in OMIM or review articles, we found, in retrospect, that craniosynostosis had indeed been described, albeit very rarely.^{25,26}

Our study describes 10 novel candidate genes, the candidacy of which is supported by multiple lines of evidence. First, the discovery of these candidates followed the same methodology we used for the other genes we identified in this study that were novel at the time of discovery but had since been confirmed by others (e.g., *WWOX*). Similarly, we have identified genes that had been independently identified by others (e.g., *C11ORF46*, *CACNA1G*, and *ZNF526*). Second, some of the novel candidates we report here are supported by compelling positional mapping data, e.g., *CDK9*, *HYAL2*, and *CTU2* (each corresponding to a novel single critical locus on autozygosity mapping). Third, the candidacy of some of these genes is supported by available animal models. For example, *Cadps* is known to play an important role in regulating glycemic

control in mouse.²⁷ Similarly, *Hyal2*-deficient mice have craniofacial anomalies reminiscent of those observed in the two patients we describe.²⁸ However, *Cacna1h*-deficient mice have no reported ptosis but rather cardiac fibrosis, which our two patients with *CACNA1H* homozygous truncation do not have.²⁹ Interestingly, heterozygous missense changes in *CACNA1H* have been associated with childhood epilepsy, but the two sisters we describe with a homozygous truncating mutation in this gene are completely normal neurologically except for ptosis.³⁰ This may suggest a different disease mechanism than we have previously shown for other genes in which biallelic loss of function results in distinct clinical phenotypes as compared with heterozygous mutations.^{9,31,32} Alternatively, the susceptibility to absence seizures may have been erroneous.

The relatively easy access to genomic sequencing tools has empowered many clinical geneticists to identify interesting novel candidate genes in their patients. However, many of these tentative links have not been published because they are typically retained until a second case with a matching phenotype and genotype is identified. Several matchmaking tools have been developed to address this bottleneck, e.g., GeneMatcher and MIMmatcher.^{33,34} Reporting detailed clinical and genomic analyses of a large series of apparently novel dysmorphology syndromes will likely lead to a trend of accelerating the establishment of novel syndromes and their underlying genes. Such a trend will catalyze matchmaking such that the proposed novel phenotype is established and its candidate gene is confirmed independently. It is only through high-throughput identification and confirmation of disease–gene links that we can reap the benefits of full medical annotation of the human genome.

SUPPLEMENTARY MATERIAL

Supplementary material is linked to the online version of the paper at <http://www.nature.com/gim>

ACKNOWLEDGMENTS

We thank the patients and their families for their enthusiastic participation. We also thank the Genotyping and Sequencing Core Facilities at KFSHRC for their technical help. This work was supported in part by a King Salman Center for Disability Research grant (F.S.A.).

DISCLOSURE

The authors declare no conflict of interest.

REFERENCES

- Aase JM. *Diagnostic Dysmorphology*. Springer: New York, 1990.
- Carey JC, Allanson JE, Hennekam RC, Biesecker LG. Standard terminology for phenotypic variations: the elements of morphology project, its current progress, and future directions. *Hum Mutat* 2012;33:781–786.
- Stessman HA, Bernier R, Eichler EE. A genotype-first approach to defining the subtypes of a complex disease. *Cell* 2014;156:872–877.
- Lupski JR. Structural variation mutagenesis of the human genome: Impact on disease and evolution. *Environ Mol Mutagen* 2015;56:419–436.
- Desai AN, Jere A. Next-generation sequencing: ready for the clinics? *Clin Genet* 2012;81:503–510.
- Boycott KM, Vanstone MR, Bulman DE, MacKenzie AE. Rare-disease genetics in the era of next-generation sequencing: discovery to translation. *Nat Rev Genet* 2013;14:681–691.
- Abu-Safieh L, Alrashed M, Anazi S, et al. Autozygome-guided exome sequencing in retinal dystrophy patients reveals pathogenetic mutations and novel candidate disease genes. *Genome Res* 2013;23:236–247.
- Aldahmesh MA, Khan AO, Mohamed JY, et al. Genomic analysis of pediatric cataract in Saudi Arabia reveals novel candidate disease genes. *Genet Med* 2012;14:955–962.
- Shaheen R, Faqeih E, Ansari S, et al. Genomic analysis of primordial dwarfism reveals novel disease genes. *Genome Res* 2014;24:291–299.
- Alazami AM, Patel N, Shamseldin HE, et al. Accelerating novel candidate gene discovery in neurogenetic disorders via whole-exome sequencing of prescreened multiplex consanguineous families. *Cell Rep* 2015;10:148–161.
- Alkuraya FS. Autozygome decoded. *Genet Med* 2010;12:765–771.
- Carr IM, Flintoff KJ, Taylor GR, Markham AF, Bonthron DT. Interactive visual analysis of SNP data for rapid autozygosity mapping in consanguineous families. *Hum Mutat* 2006;27:1041–1046.
- Alkuraya FS. Discovery of rare homozygous mutations from studies of consanguineous pedigrees. *Curr Protoc Hum Genet* 2012:Unit 6.12.
- Alkuraya FS. The application of next-generation sequencing in the autozygosity mapping of human recessive diseases. *Hum Genet* 2013;132:1197–1211.
- Najmabadi H, Hu H, Garshabi M, et al. Deep sequencing reveals 50 novel genes for recessive cognitive disorders. *Nature* 2011;478:57–63.
- Shaheen R, Ansari S, Alshammari MJ, et al. A novel syndrome of hypohidrosis and intellectual disability is linked to COG6 deficiency. *J Med Genet* 2013;50:431–436.
- Alkuraya FS, Shaheen R. Variable phenotypic expression of COG6 mutations. *J Med Genet* 2014;51:425–426.
- Synofzik M, Haack TB, Kopajtich R, et al. Absence of BiP co-chaperone DNAJC3 causes diabetes mellitus and multisystemic neurodegeneration. *Am J Hum Genet* 2014;95:689–697.
- Alkuraya FS. Arthrogryposis, perthes disease, and upward gaze palsy: a novel autosomal recessive syndromic form of arthrogryposis. *Am J Med Genet A* 2011;155A:297–300.
- Bloss CS, Zeeland AA, Topol SE, et al. A genome sequencing program for novel undiagnosed diseases. *Genet Med*; e-pub ahead of print 19 March 2015.
- Chong JX, Buckingham KJ, Jhangiani SN, et al.; Centers for Mendelian Genomics. The genetic basis of Mendelian phenotypes: discoveries, challenges, and opportunities. *Am J Hum Genet* 2015;97:199–215.
- Yavarna T, Al-Dewik N, Al-Mureikhi M, et al. High diagnostic yield of clinical exome sequencing in Middle Eastern patients with Mendelian disorders. *Hum Genet* 2015;134:967–980.
- Alkuraya FS. Mental retardation, growth retardation, unusual nose, and open mouth: an autosomal recessive entity. *Am J Med Genet A* 2010;152A:2160–2163.
- Alazami AM, Monies D, Meyer BF, et al. Congenital disorder of glycosylation IIa: the trouble with diagnosing a dysmorphic inborn error of metabolism. *Am J Med Genet A* 2012;158A:245–246.
- Courtney RJ, Pennesi ME. Retinal dystrophy in 2 brothers with α -mannosidosis. *Arch Ophthalmol* 2011;129:799–802.
- Grabb PA, Albright AL, Zitelli BJ. Multiple suture synostosis, macrocephaly, and intracranial hypertension in a child with alpha-D-mannosidase deficiency. Case report. *J Neurosurg* 1995;82:647–649.
- Speidel D, Salehi A, Obermueller S, et al. CAPS1 and CAPS2 regulate stability and recruitment of insulin granules in mouse pancreatic beta cells. *Cell Metab* 2008;7:57–67.
- Jadin L, Wu X, Ding H, et al. Skeletal and hematological anomalies in *HYAL2*-deficient mice: a second type of mucopolysaccharidosis IX? *FASEB J* 2008;22:4316–4326.
- Chen CC, Lamping KG, Nuno DW, et al. Abnormal coronary function in mice deficient in alpha1H T-type Ca²⁺ channels. *Science* 2003;302:1416–1418.
- Heron SE, Phillips HA, Mulley JC, et al. Genetic variation of *CACNA1H* in idiopathic generalized epilepsy. *Ann Neurol* 2004;55:595–596.
- Aldahmesh MA, Mohamed JY, Alkuraya HS, et al. Recessive mutations in *ELOVL4* cause ichthyosis, intellectual disability, and spastic quadriplegia. *Am J Hum Genet* 2011;89:745–750.
- Patel N, Faqeih E, Anazi S, et al. A novel APC mutation defines a second locus for Cenani–Lenz syndrome. *J Med Genet* 2015;52:317–321.
- Gottlieb MM, Arenillas DJ, Maithripala S, et al. GeneYenta: a phenotype-based rare disease case matching tool based on online dating algorithms for the acceleration of exome interpretation. *Hum Mutat* 2015;36:432–438.
- Sobreira N, Schiettecatte F, Boehm C, Valle D, Hamosh A. New tools for Mendelian disease gene identification: PhenoDB variant analysis module; and GeneMatcher, a web-based tool for linking investigators with an interest in the same gene. *Hum Mutat* 2015;36:425–431.